FÍSICA
Acta Científica Venezolana, 66(3): 145–151, 2015

STRUCTURAL AND MAGNETIC CHARACTERIZATION OF THE ALLOY SYSTEM $\mathbf{CuAl_{1-x}Cr_xS_2}$ ($x = 0.10$ **and** $x = 0.20$)

M.A. Villarreal,[1,*] P. Grima,[1] M. Quintero,[1] E. Moreno,[1]
E. Calderon,[1] G. Delgado,[2] P. Silva[3] and J. Villegas[3]
[1]Centro de Estudios en Semiconductores, Departamento de Física, ULA, Mérida, Venezuela
[2]Laboratorio de Cristalografía, Departamento de Química, ULA, Mérida, Venezuela
[3]Laboratorio de la Materia Condensada, Centro de Física, IVIC, Caracas, Venezuela

Recibido: 24/04/2015 Corregido: 14/07/2015 Aceptado: 07/08/2015

ABSTRACT The synthesis, structural characterization and magnetic properties of the alloy system $CuAl_{1-x}Cr_xS_2$ ($x = 0.10$ and $x = 0.20$) is reported. Both samples were synthesized using the direct fusion technique. Chemical analysis (EDX) confirmed the stoichiometric ratio for both concentrations. The powder diffraction patterns were indexed, and both principal phases crystallize with tetragonal symmetry and unit cell parameters $a = 5.3317(1)$ Å, $c = 10.4059(2)$ Å for $x = 0.10$ and $a = 5.3331(1)$ Å, $c = 10.4117(2)$ Å for $x = 0.20$. These materials are isomorphic with the chalcopyrite structure that crystallizes in the space group $I\bar{4}2d$. The system behaves paramagnetic for $x = 0.10$ and antiferromagnetic for $x = 0.20$ with Néel temperature ~ 20 K. The EPR linewidth and g factor are temperature independent for $x = 0.10$, while for $x = 0.20$ the linewidth follows a Korringa-like behavior ($\Delta H/\Delta T = 0.39$ mT/K) as a function of temperature. These results are discussed in terms of nearest-neighbor Cr^{+3} ($S = 3/2$) spin-coupled pairs. **Keywords:** semiconductors, X-ray diffraction, susceptibility, electron paramagnetic resonance.

CARACTERIZACIÓN ESTRUCTURAL Y MAGNÉTICA DEL SISTEMA DE ALEACIONES $\mathbf{CuAl_{1-x}Cr_xS_2}$ ($x = 0{,}10$ **y** $x = 0{,}20$)

RESUMEN En este trabajo se reporta la síntesis, caracterización y propiedades magnéticas del sistema de aleaciones $CuAl_{1-x}Cr_xS_2$ ($x = 0{,}10$ y $x = 0{,}20$). Las muestras fueron sintetizadas utilizando la técnica de fusión directa. El análisis químico (EDX) permitió establecer las relaciones estequiométricas de las muestras. El análisis por difracción de rayos-X indica que las fases principales de las aleaciones cristalizan en el sistema tetragonal con parámetros de celda $a = 5{,}3317(1)$ Å, $c = 10{,}4059(2)$ Å para $x = 0{,}10$ y $a = 5{,}3331(1)$ Å, $c = 10{,}4117(2)$ Å para $x = 0{,}20$. Estos materiales son isomorfos con la estructura calcopirita que cristaliza en el grupo espacial $I\bar{4}2d$. El sistema presenta un comportamiento paramagnético para $x = 0{,}10$ y antiferromagnético para $x = 0{,}20$ con temperatura de Néel de ~ 20 K. El ancho de línea EPR y el factor g son independientes de la temperatura para $x = 0{,}10$, mientras que para $x = 0{,}20$ el ancho de línea sigue un comportamiento tipo Korringa como función de la temperatura ($\Delta H/\Delta T = 0{,}39$ mT/K). Estos resultados se discuten en términos de los vecinos más cercanos de los pares de espín-acoplado del Cr^{+3} ($S = 3/2$). **Palabras clave:** semiconductores, difracción de rayos-X, susceptibilidad magnética, resonancia paramagnética electrónica.

INTRODUCTION

Semiconductors showing ferromagnetic ordering at room temperature have been of great interest in the last several years due their possibilities in future spintronic devices.[1] In addition to potentially relevant technological applications and interesting experimental results,[2–5] it is fundamental to focus on the electronic properties of diluted magnetic chalcopyrites (DMCHs); i.e. different chalcopyrites doped with several transition metals.

As is well known, there are two kinds of chalcopyrite: $II - IV - V_2$ and $I - III - VI_2$. The first class represents the ternary analogue of an $III - V$ semiconductor, where the element of the third column is substituted by an element of the second and fourth columns, alternately. Similarly, the second class of chalcopyrite is the ternary counterpart of the $II - VI$ semiconductor, where the cation is substituted by an element of the first and third columns, alternately. Therefore, ternaries offer a vast playground for achieving different electronic and magnetic properties due to the wide variety of sites where the transition metal (TM) can be doped; in fact, a TM can be substituted for the II and IV sites in the first class of chalcopyrite and for the I and III sites in the second class. In this respect, different TMs, with their correspondingly different number of d electrons, can have different valence states when substituted in the same chalcopyrite site.[6] In particular, Cr doped $CuAlS_2$ and $AgGaS_2$ were predicted to have a remarkably high Curie temperature (above room temperature), although the estimate was based on a mean-field theory which is well known to overestimate T_C.[7]

In order to determine the structural characterization and the magnetic behavior of these alloys, we present in this work a study of EDX, X-ray diffraction, magnetic susceptibility and electron paramagnetic resonance of the system $CuAl_{1-x}Cr_xS_2$ with $x = 0.10$ and $x = 0.20$.

SAMPLES AND MEASUREMENTS

Polycrystalline Cr-doped $CuAl_{1-x}Cr_xS_2$ ($x = 0.10$ and $x = 0.20$) samples were obtained by using the direct fusion technique. Stoichiometric quantities of the elements Cu, Al, Cr and S were charged in an evacuated and sealed quartz ampoule that was previously subjected to pyrolysis in order to avoid reaction of the starting materials with quartz. The fusion process was carried out into a furnace (vertical position) heated up to 500 °C at a rate of 50 °C/h and then heated up to 1050 °C at a rate of 20 °C/h. The ampoule was kept at this temperature for a period of 12 days. Finally, the sample was cooled to room temperature at a rate of 6 °C/h during 2 days.

Chemical analysis of the sample was carried out with a Hitachi S-2500 scanning electron microscope (SEM) equipped with a Kevex EDX accessory. For the X-ray analysis, a small quantity of the samples was ground mechanically in an agate mortar and pestle. The X-ray powder diffraction data were collected at 298(1) K in θ/θ reflection mode using a Bruker D8 diffractometer operating in Bragg–Brentano geometry, equipped with an X-ray tube (Cu K_α radiation: $\lambda = 1.54059$ Å), a nickel filter and a 1-dimensional LynxEye detector. The specimen was scanned from 10 to 100° 2θ with a step size of 0.02° and counting time of 1 s.

Measurements of susceptibility as a function of temperature in the range 2–300 K with an external magnetic field 10 mT were performed using a Quantum Design SQUID magnetometer. The EPR measurements in the alloys were carried out in an X band VARIAN spectrometer with a frequency 9.4 GHz that uses a home-made cavity in the temperature range 80–300 K.

RESULTS, ANALYSIS AND DISCUSSION

Three different regions of the ingot were scanned and the average atomic percentages — Cu (22.03%), Al (22.08%), Cr (2.76%) and S (53.13%) for $x = 0.10$ and Cu (27.16%), Al (18.58%), Cr (3.30%) and S (50.96%) for $x = 0.20$ — gave an atomic ratio close to the ideal value. Tables **1**–**2** show the data registered in these regions. In Figures **1**–**2** spectral qualitative analyses EDS for $x = 0.10$ and $x = 0.20$ are respectively shown. The results confirm that the four elements are present at the points under observation in the samples analyzed, in addition to displaying a good correlation where Al is replaced by Cr. An automatic search in the PDF-ICDD database[8] indicated that the powder patterns contain different amounts of Al_2S_3 (PDF 26-0037) for $x = 0.10$ and 0.20. The powder diffraction patterns were indexed,[9] and the principal phases crystallize with tetragonal symmetry. These compounds are isomorphic with the chalcopyrite structure which

crystallizes in the space group $I\bar{4}2d$.[10]

Element	Top region	Central region	Low region
	%Atom (error)	%Atom (error)	%Atom (error)
Cu	22.62 (0.31)	21.39 (0.31)	22.10 (0.32)
Al	21.73 (0.17)	22.20 (0.17)	22.31 (0.16)
Cr	2.69 (0.08)	2.54 (0.10)	3.04 (0.12)
S	52.96 (0.27)	53.87 (0.27)	52.55 (0.27)

Table 1: Chemical analysis for $x = 0.10$.

Element	Top region	Central region	Low region
	%Atom (error)	%Atom (error)	%Atom (error)
Cu	29.14 (0.37)	24.02 (0.36)	28.33 (0.37)
Al	16.43 (0.16)	21.17 (0.17)	18.12 (0.18)
Cr	3.62 (0.09)	3.17 (0.17)	3.12 (0.17)
S	50.81 (0.26)	51.64 (0.26)	50.43 (0.27)

Table 2: Chemical analysis for $x = 0.20$.

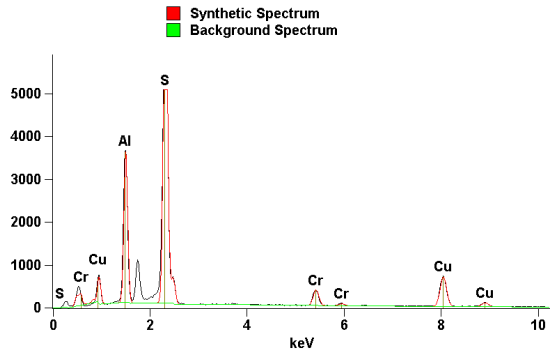

Figure 1: Spectral qualitative analysis for $x = 0.10$.

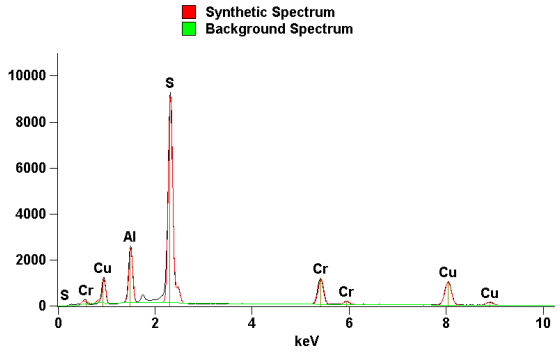

Figure 2: Spectral qualitative analysis for $x = 0.20$.

The crystal structure refinement was performed by means of the Rietveld method[11] using the Fullprof program.[12] The starting parameters were taken from the $CuAlS_2$ chalcopyrite structure.[13] The angular dependence of the peak full width at half maximum (FWHM) was described by Cagliotti's formula.[14] Peak shapes were described by the parameterized Thompson-Cox-Hastings pseudo-Voigt profile function.[15] The background variation was described by a polynomial with six coefficients. The atoms thermal motion was described by one overall isotropic temperature factor. The results of the Rietveld refinement for two compositions are summarized in Table **3**. In Figures **3**–**4** the observed, calculated and difference profile for the final cycle of Rietveld refinements for $x = 0.10$ and $x = 0.20$ are respectively shown. Atomic coordinates, fractional occupancies and isotropic temperature factors are listed in Table **4**. Bond distances for each compound are given in Table **5**.

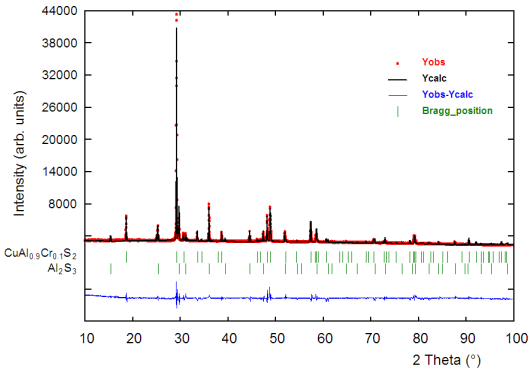

Figure 3: Rietveld refinement plot for $x = 0.10$.

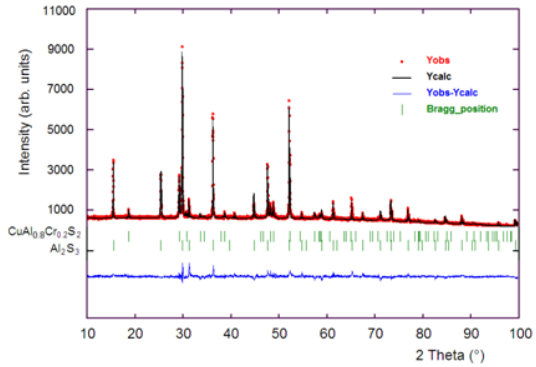

Figure 4: Rietveld refinement plot for $x = 0.20$.

In Figures **5**–**6**, the magnetic susceptibility χ as a function of temperature T for $x = 0.10$ and 0.20 are shown. The concentration $x = 0.10$ exhibits the typical behavior of a paramagnetic material, and about 140 K the ZFC and FC curves separate with decreasing temperature showing clear effects of irreversibility. The concentration $x = 0.20$ shows the characteristic behavior of an antiferromagnetic material with a Néel temperature of 20 K and hysteresis effects at very low temperatures. This result would suggest

Composition	$x = 0.10$	$x = 0.20$
molecular formula	$CuAl_{0.9}Cr_{0.1}S_2$	$CuAl_{0.8}Cr_{0.2}S_2$
molecular weight	157.16	159.66
a (Å)	5.3317 (1)	5.3331 (1)
c (Å)	10.4059 (2)	10.4117 (2)
c/a	1.95	1.95
V (Å^3)	295.81 (1)	296.13 (1)
Z	4	4
Crystal system	Tetragonal	Tetragonal
Space group	$I\bar{4}2d$ (No. 122)	$I\bar{4}2d$ (No. 122)
d_{calc} (g/cm^3)	3.53	3.58
Temperature (K)	298 (1)	298 (1)
R_p(%)	6.3	6.6
R_{wp}(%)	6.7	7.3
R_{exp}(%)	3.2	4.0
S	1.1	1.1

Table 3: Rietveld refinement results for $CuAl_{1-x}Cr_xS_2$.

	Atom	Site	x	y	z	Foc	B(Å^2)
$x = 0.10$							
	Cu	4a	0	0	0	1	0.6(1)
	Al	4b	0	0	1/2	0.89(2)	0.6(1)
	Cr	4b	0	0	1/2	0.11(2)	0.6(1)
	S	8d	0.270(1)	1/4	1/8	1	0.6(1)
$x = 0.20$							
	Cu	4a	0	0	0	1	0.8(1)
	Al	4b	0	0	1/2	0.82(2)	0.8(1)
	Cr	4b	0	0	1/2	0.18(2)	0.8(1)
	S	8d	0.267(1)	1/4	1/8	1	0.8(1)

Table 4: Atomic coordinates and isotropic temperature factors for $CuAl_{1-x}Cr_xS_2$.

	Cu–S$^{(i)}$	Al(Cr)–S$^{(ii)}$
$x = 0.10$	2.354(3)	2.230(3)
$x = 0.20$	2.345(3)	2.240(3)
Symmetry codes:	$^{(i)}y, -x, -z$	$^{(ii)}0.5 - x, y, 0.75 - z$

Table 5: Bond distances (Å) for $CuAl_{1-x}Cr_xS_2$.

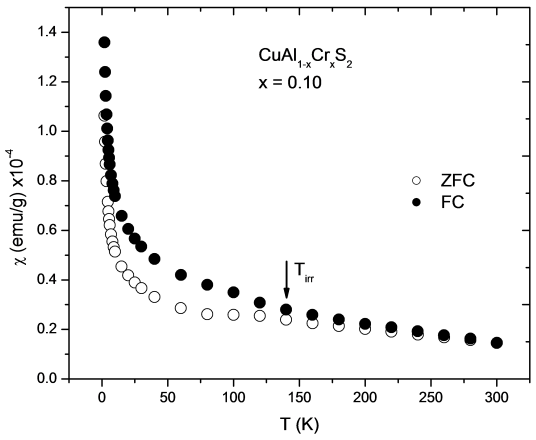

Figure 5: Temperature dependence of the magnetic susceptibility for $x = 0.10$.

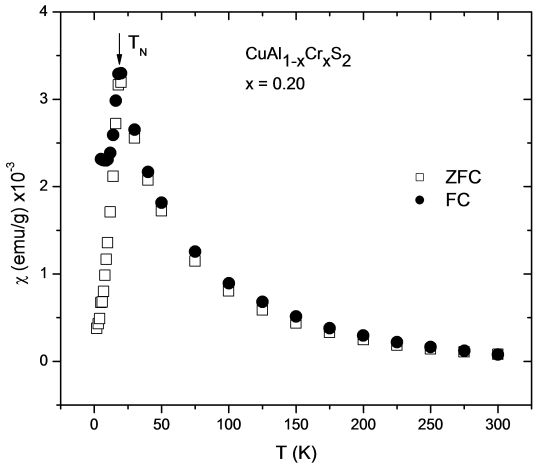

Figure 6: Temperature dependence of the magnetic susceptibility for $x = 0.20$.

that effects from anisotropy would be important in this temperature range, since in this range the thermal effects are small enough for the anisotropy to influence the spin directions when the applied field is zero or small. With a polycrystalline sample, the various crystallites can act in a way formally similar to domains and produce hysteresis effect.[16] In previous work we have studied the concentration $x = 0.33$.[17] The alloy exhibits a ferrimagnetic ordering with Néel temperature of 40 K.

The inverse of the susceptibility $1/\chi$ with temperature T (not shown) is not in accordance with a linear Curie–Weiss for $x = 0.10$ and $x = 0.20$. These results would be due to the presence of small traces of secondary phase in the respective phase of each concentration of the $CuAl_{1-x}Cr_xS_2$ system, which would lead to inaccuracies in the material mass and, hence, in the susceptibility measurements.

In Figures **7**–**8**, the temperature evolutions of the EPR spectra between 80 and 290 K for $x = 0.10$ and between 80 and 180 K for $x = 0.20$ are shown. For $x = 0.10$ the EPR spectra show a single isotropic resonance with the presence of a shoulder on the left-hand side between 80–120 K, while for $x = 0.20$ the EPR spectra show a single isotropic resonance where the intensity decreases with temperature.

In Figures **9**–**10**, the T dependence of the linewidth ΔH_{pp} and the resonance field H_r are respectively shown for each sample. For $x = 0.10$, the behavior of ΔH_{pp} is typical of a paramagnetic material, while for $x = 0.20$, ΔH_{pp} exhibits a slight variation at 200 K (paramagnetic behavior) and then a "sharp" increase up to room temperature following a Korringa-like be-

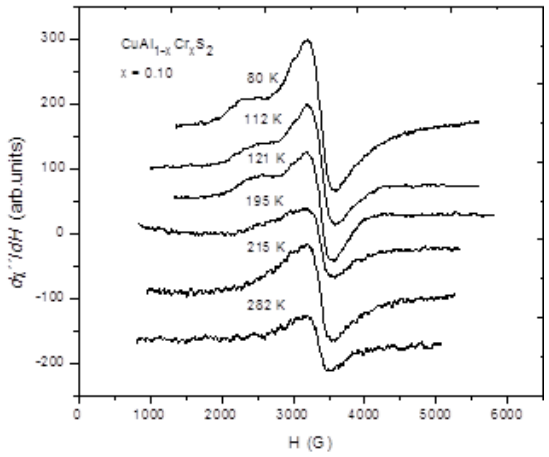

Figure 7: Temperature evolution of the EPR spectra for $x = 0.10$.

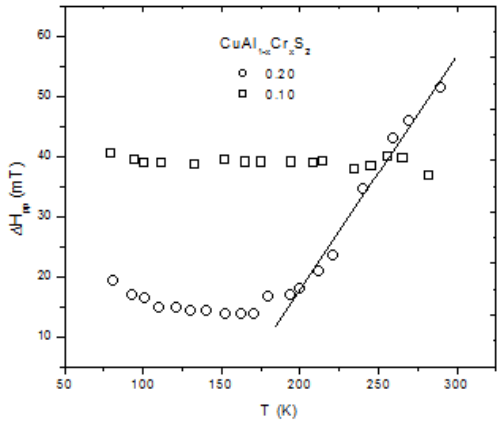

Figure 9: Temperature dependence of the EPR linewidth for $x = 0.10$ and $x = 0.20$.

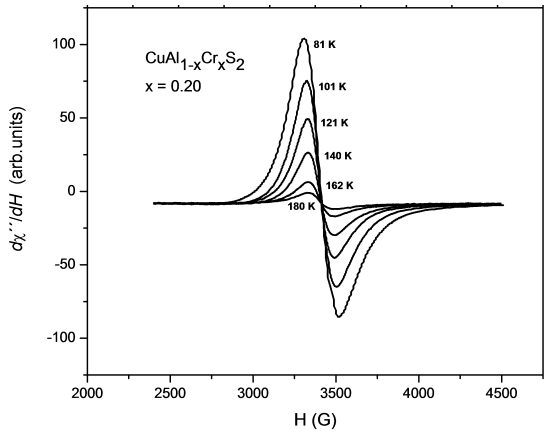

Figure 8: Temperature evolution of the EPR spectra for $x = 0.20$.

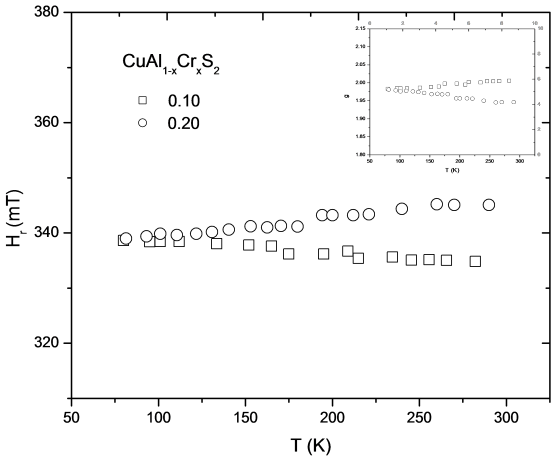

Figure 10: Temperature dependence of the resonance field for $x = 0.10$ and $x = 0.20$. The inset shows the g factor.

havior. The thermal broadening of the linewidth was fitted using $\Delta H_{pp} = a + bT$ (in the range of 190–290 K) with $a = -60.2$ mT and $b = 0.39$ mT/K. Of these results we determined the Curie–Weiss temperature $\Theta_{CW} = -154.4$ K from $\Delta H_0 = -b\Theta_{CW}$, where $\Delta H_0 = a$ is the residual linewidth.[18]

For $x = 0.10$, both the resonance field H_r and the g factor show a slight variation in the whole temperature range, and its mean value is $g = 1.99(1)$. For $x = 0.20$ it can be seen that decreasing the temperature slightly decreases H_r. In addition, we see the slope change in the temperature just where the Korringa relaxation appears, while the g factor decreases slightly to room temperature and its mean value is $g = 1.96(1)$. Values obtained for g are in the range of the particular case of Cr (III).[19]

CONCLUSIONS

The structural characterization showed that the principal phases crystallize with tetragonal symmetry and unit cell parameters $a = 5.3317(1)$ Å, $c = 10.4059(2)$ Å for $x = 0.10$ and $a = 5.3331(1)$ Å, $c = 10.4117(2)$ Å for $x = 0.20$. These materials are isomorphic with the chalcopyrite structure that crystallizes in the space group $I\bar{4}2d$. The magnetic results suggest that concentration $x = 0.10$ is paramagnetic while $x = 0.20$ shows antiferromagnetic behavior with Néel temperature ~ 20 K. In the case of $x = 0.20$ the linewidth follows a Korringa-like behavior ($\Delta H/\Delta T = 0.39$ mT/K) as a function of temperature.

ACKNOWLEDGEMENTS

This work was supported by the CDCHTA of Universidad de Los Andes through Project No. NURR-C-497-08-05-B.

REFERENCES

1. **Wolf, S.A., Chtchelkanova, A.Y., Treger, D.M.** Spintronics: A retrospective and perspective. *IBM J. Res. & Dev.*, **50**:101, 2006.

2. **Medvekin, G.A., Ishibashi, T., Nishi, T., Hiyata, K.** Room-temperature ferromagnetism in novel diluted magnetic semiconductor $Cd_{1-x}Mn_xGeP_2$. *Jpn. J. Appl. Phys.*, **39**:L949, 2000.

3. **Choi, S., Cha, G.B., Hong, S.C., Cho, S., Kim, Y., Ketterson, J.B., Jeong, S.Y., Yi, G.C.** Room-temperature ferromagnetism in chalcopyrite Mn-doped $ZnSnAs_2$ single crystals. *Solid State Commun.*, **122**:165, 2002.

4. **Cho, S., Choi, S., Cha, G.B., Hong, S.C., Kim, Y., Zhao, Y.J., Preeman, A.J., Ketterson, J.B., Kim, B.J., Choi, B.C.** Room-temperature ferromagnetism in $(Zn_{1-x}Mn_x)GeP_2$ semiconductors. *Phys. Rev. Lett.*, **88**:257203, 2002.

5. **Hwang, Y.H., Shen, S., Liu, X., Furdyna, J.K., Dobrowolska, M., Um, Y.H.** Room-temperature ferromagnetism in highly Cr-doped $II - Mn - VI$ magnetic semiconductor $Cd_{1-x-y}Mn_xCr_yTe$. *Phys. Rev. B*, **88**:075205, 2013.

6. **Sarkisov, S.Y., Picozzi,S.** Transition-metal doping of semiconducting chalcopyrites: half-metallicity and magnetism. *J. Phys: Condens. Matter*, **19**:016210, 2007.

7. **Kamatani, T., Akai, H.** The magnetic properties in transition metal-doped chalcopyrite semiconductors. *Mater. Sci. Semicond. Process.*, **6**:389, 2003.

8. **PDF-ICDD-Powder Diffraction File (Set 1-57)**. International Centre for Diffraction Data, 12 Campus Boulevard, Newton Square, PA, USA 2007.

9. **Boultif, A., Löuer, D.** Powder pattern indexing with the dichotomy method. *J. Appl. Cryst.*, **37**:724, 2004.

10. **Hall, S.R., Stewart, J.M.** The crystal structure refinement of chalcopyrite, $CuFeS_2$. *Acta Cryst. B*, **29**:579, 1973.

11. **Rietveld, H.M.** A profile refinement method for nuclear and magnetic structures. *J. Appl. Cryst.*, **2**:65, 1969.

12. **Rodríguez-Carvajal, J.** Fullprof (Version 4.0). Laboratoire Leon Brillouin (CEA, CNRS), France, 2010.

13. **Hahn, H., Frank, G., Klingler, W., Meyer, A.D., Stoercer, G.** Studies on ternary chalcogenides. About ternary chalcogenides of aluminum, gallium, indium and zinc, cadmium and mercury. *Z. Anorg. Allg. Chem.*, **271**:153, 1953.

14. **Cagliotti, G., Paoletti, A., Ricci, F.P.** Choice of collimators for a crystal spectrometer for neutron diffraction. *Nucl. Instrum.*, **3**:223, 1958.

15. **Thompson, P., Cox, D.E., Hastings, J.B.** Rietveld refinement of Debye-Scherrer synchrotron X-ray data from Al_2O_3. *J. Appl. Cryst.*, **20**:79, 1987.

16. **Quintero, E., Quintero, M., Moreno, E., Morocoima, M., Grima, P., Bocaranda, P., Henao, J.A., Pinilla, P.** Magnetic properties of $Cu_2Cd_{1-z}Mn_zGeSe_4$ and $Cu_2Cd_{1-z}Fe_zGeSe_4$ alloys. *Journal of Alloys and Compounds.*, **471**:16, 2009.

17. **Villarreal, M.A., Grima, P., Quintero, M., Moreno, E., Delgado, G. E., Fernández, J., Silva, P., Villegas, J.** Síntesis, caracterización estructural y magnética de la aleación $CuAl_{0.67}Cr_{0.33}S_2$. *Rev. LatinAm. Metal. Mat.*, **32**(2):292, 2012.

18. **Duque, J.G.S., Miranda, E., Belon, A.M.O., Bufaical, L., Rettori, C., Pagliuso, P.G.** Magnetic properties of frustrated Y-doped $GdInCu_4$. *Physica B*, **398**:430, 2007.

19. **Solano, A., Sosa, M.E.** Aplicación de un modelo para la interpretación de espectros de resonancia paramagnética electrónica de sistemas

octaédricos de Cr(III). *Revista de la Sociedad Química de México*, **44**:168, 2000.

*__Correspondence__: Manuel Antonio Villarreal, Centro de Estudios en Semiconductores, Departamento de Física, Facultad de Ciencias, Universidad de Los Andes, Sector La Hechicera, Mérida 5101, Venezuela.
Email: mavu@ula.ve